Journal of Applied Electrochemistry (2005) 35:279–283
DOI 10.1007/s10800-004-6774-7

The bromine electrode Part III: reaction kinetics at highly boron-doped diamond electrodes

SERGIO FERRO
Department of Chemistry, University of Ferrara, via L. Borsari 46, I-44100 Ferrara, Italy (e-mail: fre@unife.it)

Received 17 May 2004; accepted in revised form 12 November 2004

Key words: anodic bromide oxidation, boron-doped diamond, cathodic bromine reduction, electrode processes, electron transfer

Abstract

Bromide oxidation and bromine reduction were investigated at boron-doped diamond (BDD) electrodes, in acidic media. Both the anodic and the cathodic reactions of the bromine redox couple were found to take place through a mechanism in which the Volmer step is rate-determining, as a result of a very poor stabilization of intermediate radical species. Accordingly, exchange current densities at BDD and polycrystalline Pt differ by more than five orders of magnitude. Finally, from the analysis of CV data, estimations of the anodic and cathodic transfer coefficients, as well as of heterogeneous rate constants, were obtained.

1. Introduction

The different halogen/halide redox systems have been used as model electrochemical reactions for the characterization of new anode materials. In particular, the chlorine evolution reaction (CLER) has been extensively studied, for its industrial implications and for more fundamental scopes, related to the influence of the electrode material on its kinetics [1–5].

Anodic bromide oxidation was the subject of a more limited number of investigations, mostly performed at polycrystalline Pt electrodes. The paper by Conway and co-workers [6]. presents new insights into the reaction mechanism, in connection with the possible interference of concomitant oxygen evolution reaction intermediates. A previous paper of ours [7], on the other hand, supplies further information on the subject, especially due to the simultaneous presence of both the partners of the redox couple.

In view of the above, highly conductive, boron-doped diamond (BDD) electrodes were also considered, and a thorough investigation of the CLER at this anode material was reported [5].

Conversely, the other two halides (bromide and iodide) were scarcely investigated and, as far as the BDD electrodes are concerned, only a cyclic voltammetric analysis was carried out [8]. The halide oxidation rate is generally extremely low at BDD [8], most probably due to weak adsorption of the intermediate halogen radicals on the electrode surface [5].

In the present work, the research has been further developed to describe the mechanisms of bromide oxidation and bromine reduction, at high quality, highly conductive BDD films.

2. Experimental

Highly boron-doped diamond (BDD) electrodes were synthesized at CSEM (Neuchâtel, Switzerland) via the hot filament chemical vapor deposition technique, using a 1% CH_4 in H_2 gas mixture, containing trimethylboron as the boron source (1–3 ppm with respect to H_2). Columnar, randomly textured and conductive ($\rho = 15$ mΩ cm, $\pm 30\%$) polycrystalline diamond films were obtained. In particular, the HF-CVD process optimized at CSEM, and based on high initial nucleation densities (e.g. $> 10^{12}$ sites cm^{-2}) and highly homogeneous growth, allows synthesis of very thin diamond films (between 0.1 and 3 μm). Samples used in the present investigation were cut from a low-resistivity (1–3 mΩ cm) silicon wafer, on which a continuous *p*-diamond coating (1 μm thick, $\pm 5\%$) was grown; micro-crystals ranged in size from 0.2 to 0.8 μm and their facets were mainly $<111>$ oriented. The working electrode had a nominal surface area of 0.785 cm^2 (a disk with a diameter of 1 cm); more details on electrode preparation (cutting) and cell assembling were reported in [5]. The electrochemical behavior of the BDD electrode was tested through the investigation of different redox couples: $Fe^{3+/2+}$ and $Fe(CN)_6^{3-/4-}$ [9], $Ce^{4+/3+}$ [10]. and $Eu^{3+/2+}$ [11], showing that kinetic responses are comparable with those recorded at (oxide-free) noble-metal electrodes.

Electrochemical measurements were performed at room temperature, by means of an Autolab PGSTAT20 (EcoChemie), recording cyclic voltammetries (CV) and quasi-steady polarization curves. CV data were obtained at different scan rates (v), from 0.05 to 1.00 V s^{-1}, in solutions containing from 0.001 to 1 mol l^{-1} of both the reduced (bromide) and oxidized (bromine) partners of the redox couple. For each reactant concentration and scan rate, at least five cycles were recorded, and the last set of current-potential data was considered. Quasi-steady polarization curves were obtained both in the low-overpotential range (± 20 mV with respect to the open circuit potential, OCP), and covering a wider potential range, which extended from 1.35 to 0.00 V vs. a double-walled, saturated calomel electrode (SCE), with an intermediate saturated $NaNO_3$ solution. The former measurements were obtained at a scan rate of 0.1 mV s^{-1} and with a step potential of 0.15 mV, starting from the higher potential value and conditioning the electrode at this initial potential for 30 seconds; a scan rate of 0.5 mV s^{-1} and a step potential of 0.45 mV were chosen for the latter. In both cases, the solution was stirred by means of a peristaltic pump, withdrawing the solution in very close proximity to the electrode surface (this procedure proved to be very effective for homogenizing the solution composition and, in particular, for avoiding local pH variations [4]).

In addition to the above investigations in the proximity of the OCP, the exchange current densities were also obtained by electrochemical impedance spectroscopy; an Autolab Frequency Response Analyzer (FRA) was used, performing measurements at the OCP, in the 10^4–10^{-1} Hz frequency range and with a measuring signal amplitude of 5 mV.

Details on solution preparation were given in [7]; in all cases, the test solution was adjusted to a pH of 2 with perchloric acid, and a constant ionic strength (also equal to 2) was maintained, by adding the appropriate amount of sodium perchlorate. In addition to the BDD film, which was placed at the bottom of the electrochemical cell [5], a low-porosity graphite cylinder and the above-described SCE were used as the counter and the reference electrodes, respectively.

3. Results and Discussion

CV data for three different reactant concentrations (1, 5 and 10 mM Br^-/Br_3^-) are shown in Figure 1 and, as expected, they differ significantly from the signals obtained at polycrystalline Pt [7]. In particular, the kinetics are slower at BDD, as indicated by the larger ΔE_p and the lower peak current densities. Moreover, the oxidation seems to be less difficult than reduction, as shown by the slight asymmetry of the CV curve with respect to the equilibrium potential value (see the symbol at about 0.92 V).

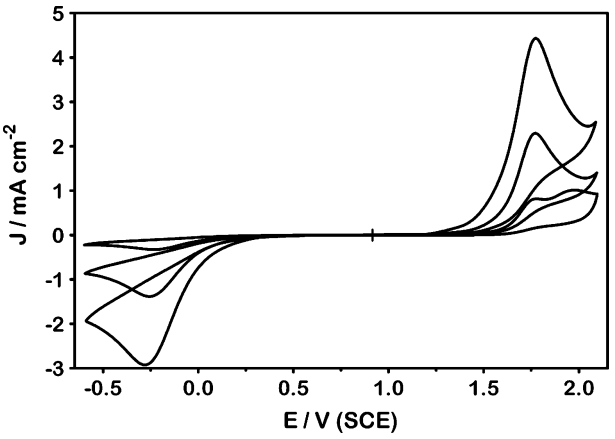

Fig. 1. CV curves for a diamond thin-film electrode in xM Br^-/xM $Br_3^-/(2-2x)$M $NaClO_4$ / 0.01M $HClO_4$ (x=0.001, 0.005 and 0.010). The cross at about 0.92 V_{SCE} corresponds to the Br^-/Br_3^- equilibrium potential value. Scan rate: 0.1 V s^{-1}.

At the lowest concentration of electroactive species, a pair of partially superimposed peaks were recorded, in the anodic part of the CV curve. The less anodic peak can be assigned to bromide oxidation, the other being possibly due to the formation of Br-related species with a higher oxidation state (e.g., hypobromites). An analogous signal was not observed for the oxidation of chlorides [5], possibly because of the narrower window of explored potentials. Accordingly, the present data may represent further support for the idea that the cathodic signals found in the potential range from 0.3 to 0.7 V in [5]. were due to hypochlorous acid. In that case, the splitting into two signals could be related to the presence of dissolved and adsorbed species, or to the pH-dependent existence of both HOCl and ClO^-. In contrast, considering again the data in [5], the reduction of dissolved chlorine would take place at potentials more negative than the chosen cathodic limit (i.e., at $E < -0.6$ V, as reported in [8]).

The peak current density, j_p, for the bromine/bromide redox couple, was found to depend linearly on $v^{1/2}$. j_p was also a linear function of the reactant concentration, in the range 1—100 mM. From the first set of measurements, estimations of the diffusion coefficient for the reactant of both the anodic and cathodic reactions were obtained: values were equal to 8.20×10^{-6} and 6.20×10^{-6} cm^2 s^{-1}, respectively. Furthermore, evaluations of transfer coefficients were performed, based on the peak potential dependence on scan rate reported in [12]. (E_p shifts of $1.15RT/\alpha n_\alpha F$ mV for each tenfold increase in v). Values of about 0.45 and 0.27 were obtained, for the anodic and cathodic transfer coefficients, in that order. Interestingly, an anodic transfer coefficient lower than 0.5 was also found for the chlorine evolution reaction [5], accounting for Tafel slopes higher than 0.120 V/decade. From the data of the present work, an estimation of transfer coefficients was also obtained considering the following equation [12], which specifically relates to the cathodic reaction (for the

oxidative one, the expression in the exponential term has the opposite sign):

$$i_{p,c} = 0.227nFAC_o^* k^0 \exp\left[-\left(\frac{\alpha n_\alpha F}{RT}\right)(E_{p,c} - E^{0'})\right] \quad (1)$$

Accordingly, plotting the logarithm of i_p (determined at different scan rates) against the difference $E_p - E^{0'}$, a linear relation is obtained, having a slope of $-\alpha n_\alpha F/RT$ and an intercept proportional to k^0. Results are shown in Figures 2a and 2b for the oxidation and reduction reactions, respectively; transfer coefficients were close to the previous values. On the other hand, kinetic constants equal to 2.14×10^{-8} and 8.10×10^{-8} cm s^{-1} were calculated, from the intercept values, for the anodic and cathodic reactions, respectively. It is important to stress that these k^0 values are determined at the respective peak potentials: they are free from concentration contributions, but still depend on potential. The usually reported value of exchange current density refers to a zero overpotential but depends on reactant concentrations.

A similar analysis was tentatively carried out on the bromine electrode data obtained at the polycrystalline Pt [7]. In that case, however, the CV investigation showed a complex behavior: as expected, the system is not as irreversible as in the present case, but not Nernstian (perfectly reversible) either. Good proportionality was found for the dependence of j_p on $v^{1/2}$ but the peak potentials were also found to depend on scan rate, which implies that treating data, based on equation (1), should only be considered an approximation, since a significant coverage by $Br^\bullet$ radicals was found at the Pt electrode, under the experimental conditions of the CV investigation [13]. Bearing in mind the above confidence limitation, values of 0.55 and 0.33, for the anodic and cathodic transfer coefficients, and 8.24×10^{-3} and 7.89×10^{-3} cm s^{-1} for the kinetic constants of the oxidation and reduction process, were found, respectively. The latter values have to be considered as underestimations, due to the uncertainties in their determination (in other words, equation 1 holds for irreversible systems, while the bromine redox equilibria at Pt behave in a quasi-reversible way). However, the difference

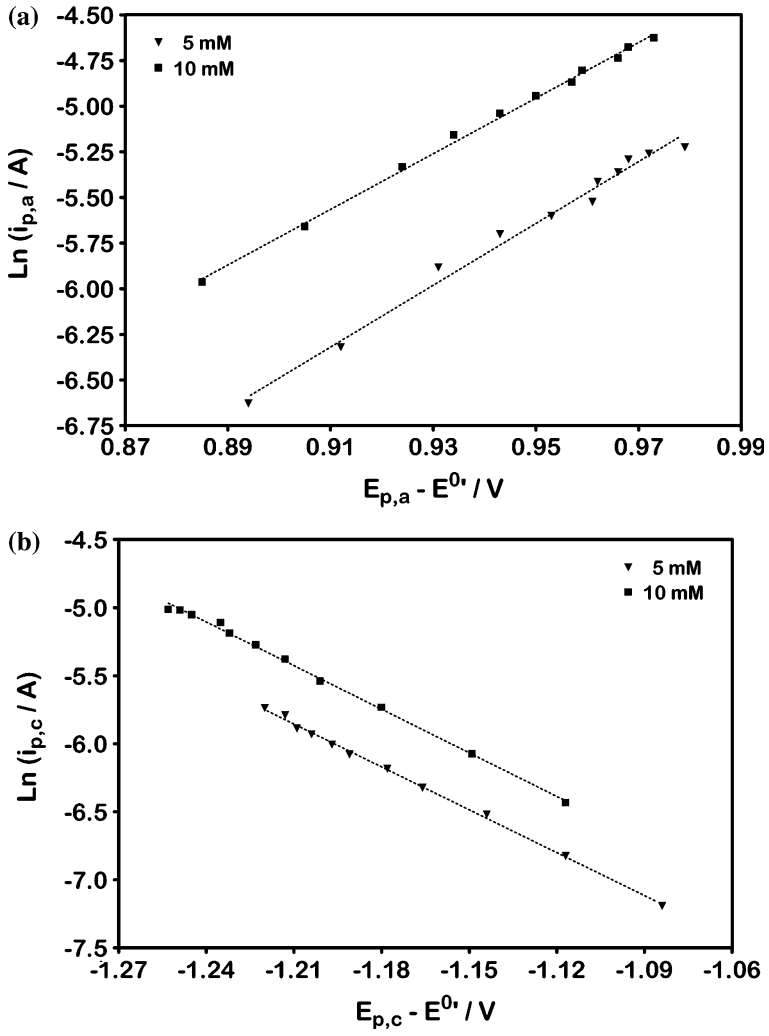

Fig. 2. Dependence of the logarithm of the peak current density versus the difference $E_p - E^{0'}$, equation 1 in the text, for the estimation of transfer coefficients and the kinetic constants [12].

between the two electrode materials is remarkable: at the Pt electrode, where reaction intermediates are certainly stabilized through adsorption [13], the reaction kinetics are five orders of magnitude larger than at BDD (where stabilizing interactions between radical intermediates and the electrode surface are nearly negligible).

For the sake of completeness of the analysis, the bromine electrode kinetics was also investigated through low-overpotential, quasi-steady polarization curves and impedance measurements, as described in the experimental section. From the slope of the j–η plots, as well as from the charge transfer resistance values obtained by frequency response analysis, estimations of the exchange current density at the different reactant concentrations were obtained, and are shown in Table 1. A reasonable concurrence exists between the two different sets of j_0 data. As confirmation of the above reported apparent kinetic constants, a difference of five or even six orders of magnitude again exists between the exchange current densities obtained at Pt and BDD, the latter being obviously more sluggish.

Quasi-steady polarization curves were also obtained over a wider potential range, i.e., exploring potential values of up to 0.5 V at both sides of the OCP, as shown in Figure 3. However, as indicated by the CV curve recorded in the 1 mM Br^-/Br_3^- solution reported in Figure 1, a positive overpotential higher than, for example, 0.2 V would allow a subsequent oxidative reaction, possibly leading to the formation of hypobromous acid. A similar problem should not exist in the cathodic part of the polarization curve, even if the alternative involvement of Br_2 and Br_3^- as the oxidized forms could justify the slight differences in slopes in Figure 3. Alternatively, the limited linearity, observed in particular for the lower redox couple concentration, could be better attributed to mass transport limitations.

Tafel slopes of 0.122–0.129 V/decade were found for both the anodic and the cathodic process, in agreement with a mechanism in which the reactant discharge is rate-determining:

$$\text{anodic reaction}\begin{cases} Br^- \rightarrow Br^\bullet + e \\ 2Br^\bullet \leftrightarrows Br_2 \end{cases} \qquad (2)$$

Table 1. Values of the exchange current density, as obtained from polarization curves (low-overpotential approximation) and impedance measurements, at different solution compositions

Br^-/Br_3^- concentration/M	$dj/d\eta$	j_0/nA cm^{-2}	R_{ct}/kΩ	j_0/nA cm^{-2}
0.001	8.247E−08	2.116	3330	9.812
0.005	1.775E−07	4.555	2358	13.86
0.010	2.929E−07	7.516	2241	14.58
0.050	5.877E−07	15.08	1622	20.14
0.100	4.283E−06	109.9	237.4	137.6
0.250	5.530E−06	141.9	230.2	141.9
0.500	7.007E−06	179.8	181.8	179.7
1.000	1.486E−05	381.3	76.3	428.2

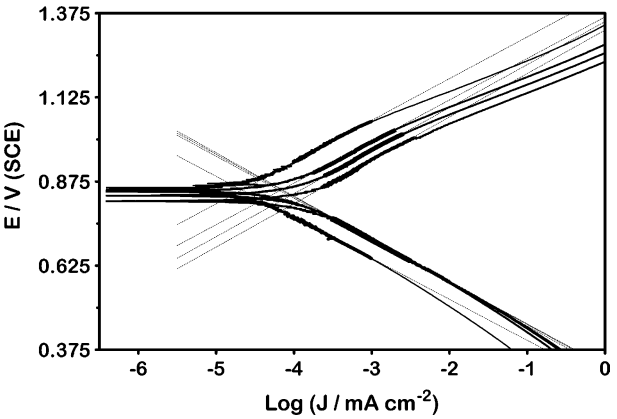

Fig. 3. Current-potential curves (Tafel plots) for the bromine electrode, recorded in xM Br^-/xM $Br_3^-/(2-2x)$M $NaClO_4$/0.01M $HClO_4$ (x from 0.1 to 1).

$$\text{cathodic reaction}\begin{cases} Br_2 + e \rightarrow Br^- + Br^\bullet \\ Br^\bullet + e \leftrightarrows Br^- \end{cases} \qquad (3)$$

The same was found for the anodic CLER at BDD 5]. Mechanisms (2) and (3) imply that the $Br^- + Br_2 \leftrightarrows Br_3^-$ equilibrium is fast, compared with the electron transfer step. As further confirmation of the above hypothesis, the log–log plots of current density against bromide concentration, at three different potentials and in the region of linearity of the relative (anodic) Tafel plots, are shown in Figure 4; as specified in the experimental part, the ionic strength of all solutions was kept constant at a value of two. A relatively good linearity was observed, with a slope of 0.94 ± 0.10, showing that the reaction is first order with respect to bromide concentration, as required by the proposed reaction mechanism. Log j vs. log c dependences were also obtained for the cathodic reaction; again, as shown in Figure 5, j values at three different potentials in the Tafel linearity region were selected. It is interesting to observe that, in spite of the lower concentration (0.1 M), a practically horizontal fit is obtained, which points to a zero reaction

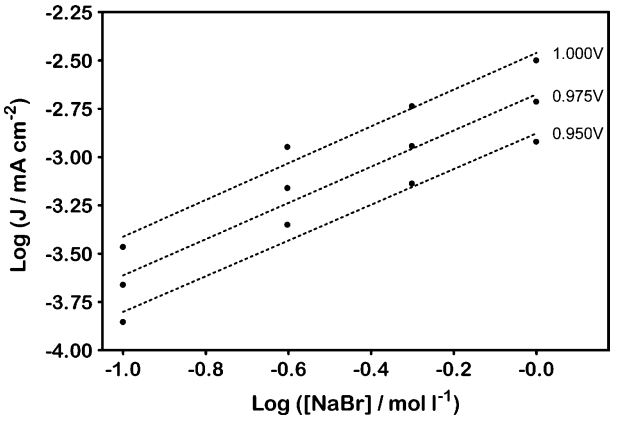

Fig. 4. Dependence of the reaction rate for the bromide oxidation on the Br^- concentration; current values were taken at different potentials in the anodic Tafel regions.

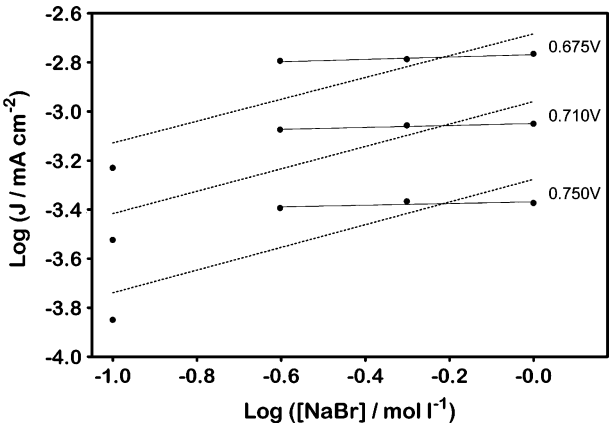

Fig. 5. Dependence of the reaction rate for the bromine reduction on the Br^- concentration (see text for details); data obtained at different potentials in the cathodic Tafel regions.

order (0.041 ± 0.019) with respect to Br_2. A detailed explanation of this result was given in [7]. In summary, because of the existence of a chemical equilibrium (whose constant is $K_{eq} = [Br_3^-]/[Br^-]\,[Br_2]$), involving the different Br-related species in solution, and due to the fact that the different solution compositions were chosen in such a way that $[Br_3^-] \approx [Br^-]$, the bromine concentration should be practically constant and equal to $(K_{eq})^{-1}$. The zero reaction order is therefore apparent, as a consequence of the imposed invariance of the reactant concentration.

4. Conclusions

Consistently with the chlorine evolution reaction [5], the anodic bromide oxidation at BDD is kinetically controlled by Br^- discharge. The same Volmer step could be suggested for the cathodic reduction of bromine (equation 3, above), thus indicating that the redox system behaves in an almost ideal way, with no intrinsic irreversibility. The very slow kinetics are therefore due to the poor adsorption of halogen radicals at the BDD surface and consequent lack of stabilization. In fact, the electrode surface cannot be considered completely indifferent, some sort of bromuration having been detected by XPS measurements [14]. However, this modification proved to be rather unstable, as confirmed by a progressive loss of bromine, under the ultra-high vacuum conditions of the XPS investigation. While such a phenomenon may have minor effects on the reaction kinetics under investigation, it is certainly of interest as far as the chemical and electrochemical inertness of diamond are concerned.

Acknowledgements

The author is indebted to Professor Achille De Battisti for stimulating this research and for helpful discussion. The valuable support of Mr. Werner Haenni and that of CSEM (Neuchâtel, CH), for providing the BDD samples, is also acknowledged.

References

1. D.M. Novak, B.V. Tilak and B.E. Conway, *in* B.E. Conway and J. O'M Bockris (Eds), Modern Aspects of Electrochemistry, Plenum Press, New York, 1982, vol. 14, p. 195.
2. A. Nidola, *in* S. Trasatti (Ed), Electrodes of Conductive Metal Oxides, Part B, Elsevier, Amsterdam, 1981, p. 627.
3. S. Trasatti and W.E. O'Grady, *in* H. Gerischer and C.W. Tobias (Eds), Advances in Electro-chemistry and Electrochemical Engineering, Wiley, New York, 1981, vol. 12, p. 177.
4. S. Ferro and A. De Battisti, *J. Phys. Chem. B* **106** (2002) 2249.
5. S. Ferro, A. De Battisti, I. Duo, Ch. Comninellis, W. Haenni and A. Perret, *J. Electrochem. Soc.* **147** (2000) 2614.
6. B.E. Conway, Y. Phillips and S.Y. Qian, *J. Chem. Soc. Faraday Trans.* **91** (1995) 283.
7. S. Ferro, C. Orsan and A. de Battisti, *J. Appl. Electrochem.* **35** (2005) 273.
8. N. Vinokur, B. Miller, Y. Avygal and R. Kalish, *J. Electrochem. Soc.* **143** (1996) L238.
9. S. Ferro and A. De Battisti, *Electrochim. Acta* **47** (2002) 1641.
10. S. Ferro and A. De Battisti, *Phys. Chem. Chem. Phys.* **4** (2002) 1915.
11. S. Ferro and A. De Battisti, *J. Electroanal. Chem.* **533** (2002) 177.
12. A.J. Bard and L.R. Faulkner, "Electrochemical methods – Fundamentals and applications", John Wiley & Sons, New York, 1980; ISBN 0–471–05542–5, pp. 215–227.
13. S. Ferro and A. De Battisti, *J. Appl. Electrochem.* **34** (2004) 981.
14. S.Ferro, M. Dal Colle and A. de Battisti, unpublished.